



Trade Science Inc.

# Organic CHEMISTRY

An Indian Journal

Full Paper

OCAIJ, 4(5), 2008 [369-374]

## Topological descriptors based quantitative structure activity relationship study of aromatic amines

P.P.Singh\*, Anil Kumar Prajapati

Department of Chemistry, M.L.K.(P.G.)College, Balrampur,U.P., (INDIA)

E-mail: dr\_ppsingh@sify.com

Received: 13<sup>th</sup> August, 2008 ; Accepted: 18<sup>th</sup> August, 2008

### ABSTRACT

QSAR study of 29 aniline derivatives whose carcinogenic activities are reported in terms of log P has been made. QSAR models have been developed with the help of descriptors, connectivity index, valence connectivity index, shape index, molecular weight, accessibility surface area and molar refractivity. Thirty-eight models have been found to have high degree of predictive power with regression coefficient above 0.9 and 12 models above 0.9597. The combination of descriptors providing the best model is log P, valence connectivity index, shape index and molecular weight.

© 2008 Trade Science Inc. - INDIA

### KEYWORDS

QSAR;  
Aniline derivatives;  
Valence connectivity index;  
Molar refractivity;  
Shape index.

### INTRODUCTION

Aromatic amines<sup>[1]</sup> are common contaminant in several working environments, including the chemical and mechanical industries. Arylamines based dyes are widely used in textile industries and cosmetics<sup>[2]</sup>. The wide use of aromatic amines together with the presence of relatively very high exposure permitted the development of epidemiological knowledge unparalleled for other chemical classes. Although the major concern posed by aromatic amines derives from carcinogenic potential, the number of QSAR studies is quite limited<sup>[3]</sup>, hence needs a comprehensive study on QSAR of aromatic amines whose biological activity is reported. Recently sets of quantum chemical descriptors have been used by us for QSAR studies of testosterone and estrogen derivatives<sup>[4-8]</sup> and topological descriptors<sup>[9]</sup> for study of toxicity of alcohols. In this paper we report QSAR studies on carcinogenicity of aromatic amines with the help of topological descriptors. The quality of QSAR has been evaluated by multi linear regression analysis.

### MATERIAL AND METHOD

The study materials of this paper are derivatives of aniline and are presented in TABLE 1 along with their carcinogenic activity in term of log P. For QSAR prediction, the 3D modeling and geometry optimization<sup>[10-11]</sup> of all the compounds have been done with the help of Cache software using the semiempirical PM3 Hamiltonian. The values of various descriptors have been calculated using Cache Software.

Regression analysis has been made by Project Leader Program associated with Pro software of Fujitsu. The values of descriptors that have been used for QSAR model have been evaluated using the same software by PM3 Hamiltonian method. The descriptors that have been used are defined below:

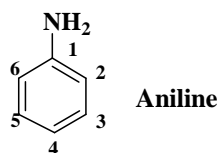
The Vertex-Connectivity Index,  $\chi = \chi(G)$ , of a (molecular) graph G is defined as<sup>[12]</sup>:

$$\chi = \sum_{\text{edges}} [d(v_i) d(v_j)]^{1/2} \quad (1)$$

The sum is taken over all edges of G;  $d(v_i)$  is the

## Full Paper

**TABLE 1: Derivatives of aniline (along with their biological activity in term of log P)**



| Compd. no. | Substituents at ring                       | Substituents at functional amino group | Activity |
|------------|--|--|----------|
| 1          | 2-Me                                       | H                                      | 1.730    |
| 2          | 2-OEt, 5-NHCOMe                            | H                                      | 0.200    |
| 3          | 3-NO <sub>2</sub> , 4-OH                   | H                                      | 0.930    |
| 4          | H  | H                                      | 1.260    |
| 5          | 2-Ome                                      | H                                      | 1.010    |
| 6          | 4-Cl                                       | H                                      | 1.780    |
| 7          | 2Cl, 5-NH <sub>2</sub>                     | H                                      | 1.000    |
| 8          | 2NH <sub>2</sub> , 4Cl                     | H                                      | 1.000    |
| 9          | 2Me, 4-OMe                                 | H                                      | 1.000    |
| 10         | 2-OMe, 5-Me                                | H                                      | 1.480    |
| 11         | 2-OMe, 5-NH <sub>2</sub>                   | H                                      | 0.230    |
| 12         | 3-NO <sub>2</sub> , 4-OEt                  | COMe                                   | 0.940    |
| 13         | 2-OMe, 5-NO <sub>2</sub>                   | H                                      | 0.960    |
| 14         | 2-NO <sub>2</sub> , 4-NH <sub>2</sub>      | H                                      | 0.430    |
| 15         | 2,4,5-Me <sub>3</sub>                      | H                                      | 2.670    |
| 16         | 2-OH, 4-NO <sub>2</sub>                    | H                                      | 0.930    |
| 17         | 2-OH, 5-NO <sub>2</sub>                    | H                                      | 0.200    |
| 18         | 4-OEt                                      | COMe                                   | 0.990    |
| 19         | 4-F  | Me, NO                                 | 1.830    |
| 20         | H  | Me, NO                                 | 1.690    |
| 21         | 2-NH <sub>2</sub>                          | H                                      | 0.480    |
| 22         | 2,4,5,6-F <sub>4</sub> , 3-NH <sub>2</sub> | H                                      | 1.040    |
| 23         | 2,4,6-Me <sub>3</sub>                      | H                                      | 2.670    |
| 24         | H  | Me                                     | 1.840    |
| 25         | 4-Me                                       | H                                      | 1.730    |
| 26         | 2-OH, 5-NO <sub>2</sub>                    | H                                      | 0.930    |
| 27         | 2,4,6-Cl <sub>3</sub>                      | H                                      | 2.820    |
| 28         | 3-Me                                       | H                                      | 1.730    |
| 29         | 2,5-Cl <sub>2</sub> , 3-COOH               | H                                      | 2.000    |

vertex-degree and  $[d(v_i) d(v_j)]^{-1/2}$  is the weight of the *i-j* edge. The degree of a vertex  $v_i$ ,  $d(v_i)$ , is equal to the number of adjacent vertices. Two vertices of graph *G* are adjacent if there is an edge joining them.

In the case of heterosystems, the connectivity index is given in terms of valence delta values  $\delta(v_i)$  and  $\delta(v_j)$  of atom *i* and *j*. This kind of connectivity index (valence-connectivity index,  $\chi_v$ ) is defined as:

$$W = (1/2) \sum_{ij} [\delta(v_i) \delta(v_j)]^{-1/2} \quad (2)$$

Valence delta values are available for many kind of atom. The connectivity index can be generalized to include also the weighted paths *pe* of length *l*, not only the weight edges (weighted path *pl* of length one):<sup>[13,14]</sup>

$${}^l\chi = \sum_{\text{paths}} [d(v_1) d(v_2) \dots d(v_{l+1})]^{-1/2} \quad (3)$$

Where  $d(v_1) d(v_2) \dots d(v_{l+1})$  are valences of vertices  $d(v_1) d(v_2) \dots, v_{l+1}$  in the considered path of length *l*. The first-,  ${}^1\chi_v$ , second-,  ${}^2\chi_v$ , and third-order,  ${}^3\chi_v$ , valence-connectivity indices in this paper are calculated by Eq. (3) when valence delta are introduced into it for heterosystems.

### Shape index

Shape index quantifying the shape of a chemical sample<sup>[15]</sup>. The shape index of order 1 (Kappa 1) quantifies the number of cycles in the chemical sample.

### Solvent accessible surface (SAS) area

The solvent accessible surface (SAS) area is calculated at an optimized geometry in water, the water geometry is from optimization first using Augmented MM2, then using MOPAC with PM3 parameters and the conductor like screening Model (COSMO)<sup>[16]</sup>.

### Molar refractivity

Molar refractivity is calculated using the atom-typing SCHEME of Ghose and Crippen<sup>[17]</sup>.

### Log P

Log P is calculated using the atom-typing scheme of Ghose and Crippen<sup>[17]</sup>.

Finally a more general but important property of chemical system is the molecular weight (MW), which has been tested as descriptors

## RESULT AND DISCUSSION

The values of the descriptors of aniline derivatives obtained by PM3 calculations are included in TABLE 2. With the help of these values 90 QSAR models using different combination of descriptors have been tried, out of which 38 models provided regression coefficient above 0.9 and 12 models above 0.9597. The predicted activities of the 12 models (PA1-PA12) are included in TABLE 3 and the regression equation developed with the values of descriptors are given below:

$$\text{PA1} = 0.876556 * \text{LPC} + 0.0820655 * \text{VCI} - 0.168902 * \text{SI} + 0.00591286 * \text{MW} + 0.00734093$$

$$r_{CV}^2 = 0.934529$$

$$r^2 = 0.968689$$

$$\text{PA2} = 0.901787 * \text{LPC} + 0.129689 * \text{SI} + 0.00591284 * \text{MW} + 0.0044592 * \text{MR} - 0.0155747$$

$$r_{CV}^2 = 0.927442$$

TABLE 2: Values of descriptors of aniline derivatives

| S.no. of compd. | Log P calcd. | Connectivity index | Valence connectivity index | Shape index | Molecular weight | Solvent accessibility surface area | Molar Refractivity |
|-----------------|--------------|--------------------|----------------------------|-------------|------------------|------------------------------------|--------------------|
| 1               | 1.731        | 3.805              | 4.887                      | 5.319       | 107.000          | 69.000                             | 35.800             |
| 2               | 0.202        | 6.630              | 8.333                      | 10.848      | 194.000          | 105.000                            | 55.051             |
| 3               | 1.027        | 5.236              | 5.520                      | 7.803       | 154.000          | 82.000                             | 39.376             |
| 4               | 1.263        | 3.394              | 3.964                      | 4.342       | 93.000           | 62.000                             | 30.758             |
| 5               | 1.011        | 4.343              | 5.295                      | 6.263       | 123.000          | 74.000                             | 37.222             |
| 6               | 1.781        | 3.788              | 5.021                      | 5.604       | 128.000          | 74.000                             | 35.563             |
| 7               | 0.998        | 4.198              | 5.521                      | 6.549       | 143.000          | 78.000                             | 40.264             |
| 8               | 0.998        | 4.198              | 5.521                      | 6.549       | 143.000          | 79.000                             | 40.264             |
| 9               | 0.758        | 5.274              | 6.626                      | 8.199       | 153.000          | 85.000                             | 43.685             |
| 10              | 1.478        | 4.736              | 6.218                      | 7.249       | 390.000          | 81.000                             | 42.263             |
| 11              | 0.227        | 4.736              | 5.795                      | 7.210       | 138.169          | 80.000                             | 41.922             |
| 12              | 1.033        | 7.668              | 9.019                      | 12.440      | 224.216          | 114.000                            | 57.275             |
| 13              | 1.058        | 5.774              | 6.481                      | 8.793       | 168.192          | 89.000                             | 44.145             |
| 14              | 0.053        | 5.236              | 5.650                      | 7.803       | 153.140          | 83.000                             | 42.382             |
| 15              | 2.665        | 4.609              | 6.732                      | 7.289       | 135.208          | 81.000                             | 45.882             |
| 16              | 1.027        | 5.236              | 5.520                      | 7.803       | 154.125          | 81.000                             | 39.376             |
| 17              | 0.196        | 4.198              | 4.834                      | 6.223       | 124.142          | 72.000                             | 37.153             |
| 18              | 0.985        | 6.220              | 7.833                      | 9.895       | 179.218          | 101.000                            | 50.351             |
| 19              | 1.830        | 5.236              | 5.990                      | 7.813       | 154.144          | 82.000                             | 40.045             |
| 20              | 1.691        | 4.843              | 5.689                      | 6.894       | 136.153          | 78.000                             | 39.828             |
| 21              | 0.480        | 3.805              | 4.464                      | 5.280       | 108.143          | 68.000                             | 35.459             |
| 22              | 1.038        | 5.464              | 5.667                      | 8.992       | 180.105          | 79.000                             | 36.324             |
| 23              | 2.665        | 4.609              | 6.732                      | 7.289       | 135.208          | 82.000                             | 45.882             |
| 24              | 2.311        | 4.305              | 5.834                      | 6.302       | 121.182          | 75.000                             | 40.487             |
| 25              | 1.731        | 3.788              | 4.887                      | 5.319       | 107.155          | 70.000                             | 35.800             |
| 26              | 1.027        | 5.236              | 5.520                      | 7.803       | 154.125          | 82.000                             | 39.376             |
| 27              | 2.817        | 4.609              | 7.134                      | 8.150       | 196.463          | 94.000                             | 45.173             |
| 28              | 1.431        | 3.788              | 4.887                      | 5.319       | 107.155          | 70.000                             | 35.800             |
| 29              | 1.998        | 5.520              | 7.355                      | 9.478       | 206.028          | 96.000                             | 47.126             |

TABLE 3: Predicted activities PA1 to PA12 of compound

| S. no. of compd. | PA1   | PA2   | PA3   | PA4   | PA5   | PA6   | PA7   | PA8   | PA9   | PA10  | PA11  | PA12  |
|------------------|-------|-------|-------|-------|-------|-------|-------|-------|-------|-------|-------|-------|
| 1                | 1.661 | 1.651 | 1.647 | 1.639 | 1.639 | 1.625 | 1.667 | 1.626 | 1.686 | 1.683 | 1.68  | 1.68  |
| 2                | 0.185 | 0.159 | 0.141 | 0.156 | 0.152 | 0.278 | 0.172 | 0.19  | 0.275 | 0.275 | 0.283 | 0.284 |
| 3                | 0.954 | 0.989 | 1.011 | 1.006 | 1.008 | 0.947 | 0.999 | 1.02  | 0.932 | 0.938 | 0.934 | 0.934 |
| 4                | 1.257 | 1.251 | 1.255 | 1.244 | 1.245 | 1.189 | 1.239 | 1.21  | 1.25  | 1.252 | 1.247 | 1.247 |
| 5                | 0.998 | 0.981 | 0.982 | 0.978 | 0.978 | 0.967 | 1.005 | 0.974 | 1.025 | 1.021 | 1.02  | 1.02  |
| 6                | 1.789 | 1.78  | 1.785 | 1.787 | 1.786 | 1.733 | 1.698 | 1.733 | 1.71  | 1.717 | 1.717 | 1.717 |
| 7                | 1.072 | 1.062 | 1.052 | 1.062 | 1.061 | 1.073 | 0.995 | 1.032 | 1.007 | 1.007 | 1.012 | 1.012 |
| 8                | 1.072 | 1.062 | 1.052 | 1.062 | 1.061 | 1.073 | 0.979 | 1.026 | 1.004 | 1.007 | 1.012 | 1.012 |
| 9                | 0.736 | 0.709 | 0.706 | 0.709 | 0.71  | 0.749 | 0.777 | 0.742 | 0.799 | 0.789 | 0.792 | 0.793 |
| 10               | 1.253 | 1.224 | 1.193 | 1.167 | 1.169 | 1.113 | 1.21  | 1.079 | 1.125 | 1.117 | 1.107 | 1.106 |
| 11               | 0.282 | 0.262 | 0.248 | 0.254 | 0.253 | 0.31  | 0.275 | 0.264 | 0.317 | 0.311 | 0.315 | 0.315 |
| 12               | 0.878 | 0.889 | 0.901 | 0.907 | 0.906 | 0.946 | 0.922 | 0.954 | 0.947 | 0.956 | 0.957 | 0.957 |
| 13               | 0.976 | 0.994 | 1.009 | 1.006 | 1.007 | 0.978 | 1.018 | 1.025 | 0.988 | 0.992 | 0.99  | 0.99  |
| 14               | 0.521 | 0.547 | 0.551 | 0.55  | 0.55  | 0.539 | 0.526 | 0.551 | 0.508 | 0.514 | 0.513 | 0.512 |
| 15               | 2.464 | 2.45  | 2.429 | 2.426 | 2.427 | 2.501 | 2.532 | 2.463 | 2.559 | 2.544 | 2.545 | 2.545 |
| 16               | 0.954 | 0.989 | 1.011 | 1.006 | 1.008 | 0.947 | 1.001 | 1.021 | 0.933 | 0.938 | 0.934 | 0.934 |
| 17               | 0.259 | 0.257 | 0.249 | 0.253 | 0.253 | 0.28  | 0.255 | 0.258 | 0.261 | 0.257 | 0.259 | 0.259 |
| 18               | 0.902 | 0.879 | 0.875 | 0.882 | 0.878 | 0.938 | 0.878 | 0.891 | 0.979 | 0.986 | 0.989 | 0.99  |
| 19               | 1.695 | 1.715 | 1.74  | 1.73  | 1.733 | 1.659 | 1.77  | 1.752 | 1.695 | 1.694 | 1.689 | 1.689 |
| 20               | 1.597 | 1.601 | 1.612 | 1.6   | 1.601 | 1.546 | 1.62  | 1.59  | 1.611 | 1.613 | 1.608 | 1.608 |
| 21               | 0.542 | 0.533 | 0.523 | 0.521 | 0.52  | 0.529 | 0.517 | 0.502 | 0.545 | 0.543 | 0.543 | 0.543 |
| 22               | 0.935 | 0.991 | 1.036 | 1.038 | 1.049 | 0.967 | 1.164 | 1.165 | 0.891 | 0.866 | 0.867 | 0.867 |
| 23               | 2.464 | 2.45  | 2.429 | 2.426 | 2.427 | 2.501 | 2.522 | 2.458 | 2.557 | 2.544 | 2.545 | 2.545 |
| 24               | 2.164 | 2.151 | 2.144 | 2.135 | 2.136 | 2.142 | 2.208 | 2.142 | 2.225 | 2.217 | 2.215 | 2.215 |
| 25               | 1.661 | 1.651 | 1.647 | 1.64  | 1.639 | 1.628 | 1.652 | 1.621 | 1.683 | 1.683 | 1.68  | 1.68  |
| 26               | 0.954 | 0.989 | 1.011 | 1.006 | 1.008 | 0.947 | 0.997 | 1.02  | 0.932 | 0.938 | 0.934 | 0.934 |
| 27               | 2.848 | 2.836 | 2.844 | 2.867 | 2.865 | 2.816 | 2.674 | 2.801 | 2.638 | 2.646 | 2.654 | 2.654 |
| 28               | 1.661 | 1.651 | 1.647 | 1.64  | 1.639 | 1.628 | 1.653 | 1.621 | 1.684 | 1.683 | 1.68  | 1.68  |
| 29               | 1.98  | 1.99  | 2.005 | 2.022 | 2.023 | 1.993 | 1.933 | 2.023 | 1.848 | 1.848 | 1.854 | 1.854 |

## Full Paper

**TABLE 4: Good QSAR models with regression coefficient ( $r^2$ ) cross-validation coefficient ( $r_{CV}^2$ ) and descriptors used**

| S. no. | Predicted activity | $r_{CV}^2$ | $r^2$    | Descriptors used  |
|--------|--------------------|------------|----------|---|
| 1      | PA1                | 0.934529   | 0.968689 | Log P calcd., valence connectivity index, shape index, Molecular weight                                     |
| 2      | PA2                | 0.927442   | 0.966753 | Log P calcd., shape index, Molecular weight, molar refractivity   |
| 3      | PA3                | 0.921406   | 0.966175 | Log P calcd., connectivity index, shape index, Molecular weight   |
| 4      | PA4                | 0.925457   | 0.965999 | Log P calcd., shape index, Molecular weight, solvent accessibility surface area                             |
| 5      | PA5                | 0.926311   | 0.965985 | Log P calcd., shape index, Molecular weight   |
| 6      | PA6                | 0.91164    | 0.96217  | Log P calcd., connectivity index, Molecular weight, molar refractivity                                      |
| 7      | PA7                | 0.906737   | 0.96158  | Log P calcd., valence connectivity index, shape index, Molecular weight, solvent accessibility surface area |
| 8      | PA8                | 0.901344   | 0.960846 | Log P calcd., connectivity index, Molecular weight, solvent accessibility surface area                      |
| 9      | PA9                | 0.891479   | 0.960463 | Log P calcd., valence connectivity index, shape index, Molecular weight, solvent accessibility surface area |
| 10     | PA10               | 0.899623   | 0.960463 | Log P calcd., valence connectivity index, shape index, solvent accessibility surface area                   |
| 11     | PA11               | 0.908388   | 0.960287 | Log P calcd., valence connectivity index, shape index   |
| 12     | PA12               | 0.889986   | 0.960287 | Log P calcd., valence connectivity index, shape index, molar refractivity                                   |

$r^2 = 0.966753$

$PA3 = 0.908926 * LPC + 0.0323916 * CI - 0.139629 * SI + 0.00647117 * MW + 0.000242272$

$r_{CV}^2 = 0.921406$

$r^2 = 0.966175$

$PA4 = 0.902819 * LPC - 0.127606 * SI + 0.00657045 * MW + 0.000832663 * SASA - 0.00595157$

$r_{CV}^2 = 0.925457$

$r^2 = 0.965999$

$PA5 = 0.904117 * LPC - 0.12361 * SI + 0.00663844 * MW + 0.0209738$

$r_{CV}^2 = 0.926311$

$r^2 = 0.965985$

$PA6 = 0.876544 * LPC - 0.170017 * CI + 0.00308498 * MW$

**TABLE 5: Values of observed activity, predicted activity and the difference between these two activities**

| S. no. of compound | Predicted activity PA1 | Observed activity | Difference |
|--------------------|------------------------|-------------------|------------|
| 1                  | 1.661                  | 1.730             | 0.069      |
| 2                  | 0.185                  | 0.200             | 0.015      |
| 3                  | 0.954                  | 0.930             | -0.024     |
| 4                  | 1.257                  | 1.260             | 0.003      |
| 5                  | 0.998                  | 1.010             | 0.012      |
| 6                  | 1.789                  | 1.780             | -0.009     |
| 7                  | 1.072                  | 1.000             | -0.072     |
| 8                  | 1.072                  | 1.000             | -0.072     |
| 9                  | 0.736                  | 1.000             | 0.264      |
| 10                 | 1.253                  | 1.310             | 0.057      |
| 11                 | 0.282                  | 0.230             | -0.052     |
| 12                 | 0.878                  | 0.940             | 0.062      |
| 13                 | 0.976                  | 0.960             | -0.016     |
| 14                 | 0.521                  | 0.430             | -0.091     |
| 15                 | 2.464                  | 2.670             | 0.206      |
| 16                 | 0.954                  | 0.930             | -0.024     |
| 17                 | 0.259                  | 0.200             | -0.059     |
| 18                 | 0.902                  | 0.990             | 0.088      |
| 19                 | 1.695                  | 1.830             | 0.135      |
| 20                 | 1.597                  | 1.690             | 0.093      |
| 21                 | 0.542                  | 0.480             | -0.062     |
| 22                 | 0.935                  | 1.040             | 0.105      |
| 23                 | 2.464                  | 2.670             | 0.206      |
| 24                 | 2.164                  | 1.840             | -0.324     |
| 25                 | 1.661                  | 1.730             | 0.069      |
| 26                 | 0.954                  | 0.930             | -0.024     |
| 27                 | 2.848                  | 2.820             | -0.028     |
| 28                 | 1.661                  | 1.730             | 0.069      |
| 29                 | 1.980                  | 2.000             | 0.020      |

$+0.0106198 * MR + 0.0443503$

$r_{CV}^2 = 0.91164$

$r^2 = 0.96217$

$PA7 = .910534 * LPC + 0.0818986 * VCI + 0.00340623 * MW$

$+ 0.0187376 * SASA + 0.615617$

$r_{CV}^2 = 0.906737$

$r^2 = 0.96158$

$PA8 = 0.909616 * LPC - 0.0660378 * CI + 0.00486398 * MW -$

$0.00776071 * SASA + 0.315788$

$r_{CV}^2 = 0.901344$

$r^2 = 0.960846$

$PA9 = 0.874749 * LPC + 0.128346 * VCI - 0.0702169 * SI -$

$0.0035159 * SASA + 0.160653$

$r_{CV}^2 = 0.891479$

$r^2 = 0.960463$

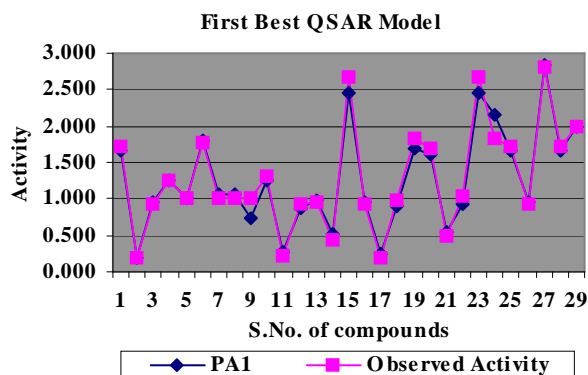
$PA10 = 0.877748 * LPC + 0.0160929 * CI + 0.109343 * VCI -$

$0.0883073 * SI + 0.0381659$

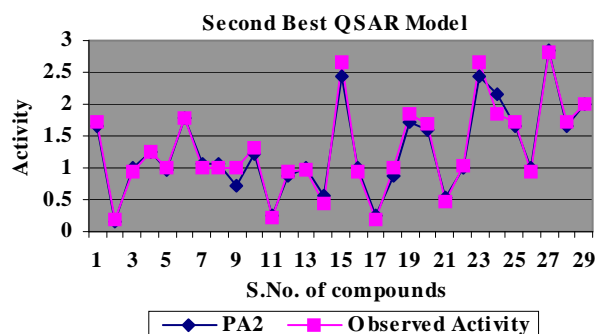
$r_{CV}^2 = 0.899623$

$r^2 = 0.960329$

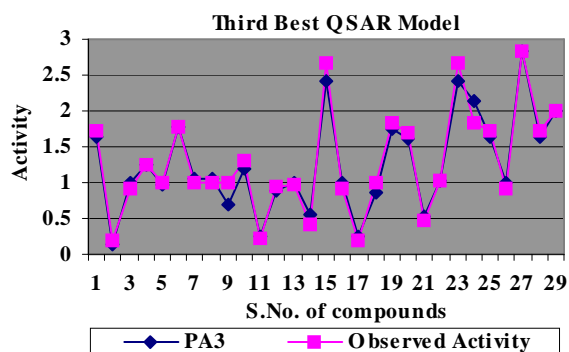
$PA11 = 0.874079 * LPC + 0.113356 * VCI - 0.081681 * SI +$



Graph 1: Graph between predicted activity PA1 and observed activity



Graph 2: Graph between predicted activity PA2 and observed activity



Graph 3: Graph between predicted activity PA3 and observed activity

0.0481882

$rCV^2 = 0.908388$

$r^2 = 0.960287$

$PA12 = 0.873820 * LPC + 0.114395 * VCI - 0.0819386 * SI - 0.00011381 * MR + 0.0490193$

$rCV^2 = 0.889986$

$r^2 = 0.960287$

On the basis of the values of regression coefficient, the QSAR models have been arranged in decreasing order of quality of prediction and are included in TABLE 4.

The predicted activity PA1 gives best QSAR mod-

els with regression coefficient 0.968689 and cross validation coefficient 0.934529. With the help of these MLR equations, the activity of aniline derivatives can be best predicted. In all the above QSAR models, the first descriptor is Log P. Even the single descriptor LPC provides good predictive power. The descriptor LPC is supposed to be the prime descriptor for QSAR models. The predicted activities and the observed activity are included in TABLE 5. The closeness between the predicted activity PA1-PA3 and the observed activity is well demonstrated by the graphs drawn between the two activities in Graph1-3.

In the second best QSAR model the descriptors are log P calcd., shape index, molecular weight and molar refractivity. In this case the predicted activity is PA2 and is given by:

$PA2 = 0.901787 * LPC + 0.129689 * SI + 0.00591284 * MW + 0.0044592 * MR - 0.0155747$

$rCV^2 = 0.927442$

$r^2 = 0.966753$

Graph between predicted activity and observed activity PA2 of the compounds of aniline derivatives is shown in the Graph-2.

In the third best QSAR model the combination of descriptor are Log P, connectivity index, shape index and molecular weight. In this case the predicted activity is given by PA3.

$PA3 = 0.908926 * LPC + 0.0323916 * CI - 0.139629 * SI + 0.00647117 * MW + 0.000242272$

$rCV^2 = 0.921406$

$r^2 = 0.966175$

## REFERENCES

- [1] D.Y.Lai, Y.T.Woo, M.F.Argus, J.C.Arcos, S.C. DeVito, R.L.Garrett; American Chemical Society: Washington, D.C., 1-13 (1996).
- [2] H.Bartsch, C.Malaveille, M.Friesen, F.F.Kadlubar; Vineis.P.Eur.J.Cancer, **29A**, 1199-1207 (1993).
- [3] R.Benigni, A.Giutiani, R.Franke, A.Gruska; Chem.Rev., **100**, 3697 (2000).
- [4] P.P.Singh, F.A.Pasha, H.K.Srivastava; QSAR and Comb.Sci., **22**, 843 (2003).
- [5] P.P.Singh, H.K.Srivastava, F.A.Pasha; Bioorg.Med. Chem., **12**, 171 (2004).
- [6] P.P.Singh, F.A.Pasha, H.K.Srivastava; Indian J.Chem.B., **43B**, 983-991 (2004).
- [7] F.A.Pasha, H.K.Srivastava, P.P.Singh; Mol.Diver.,

**Full Paper**

- 9(1-3), 215 (2005).
- [8] H.K.Srivastava, F.A.Pasha, P.P.Singh; Int.J. Quan.Chem., **103**, 237 (2005).
- [9] R.K.Singh, A.K.R.Khan, V.K.Sahu, P.P.Singh; Int.J.Quan.Chem., **108**, (2008).
- [10] M.C.Flanigan, A.Komornicki, J.W.Mciver; 'Modern Theoretical Chemistry Plenum Press', New York, 8 (1977).
- [11] M.J.S.Dewar, H.S.Rzepa, J.Am.Chem.Soc., **100**, 777 (1978).
- [12] L.B.Kier, L.H.Hall, W.J.Murray, M.Randic; J. Pharm.Sci., 65 (1976).
- [13] M.Randic, S.Sabljić, S.Nikolic, N.Trinajstić; Int.J. Quantum.Chem., Quantum Biol.Symp., **15**, 267 (1988).
- [14] S.Nikolic, M.Medic-Saric, Matijević-Soca; Croat. Chem.Acta, 66 (1993).
- [15] L.H.Hall, L.B.Kier, K.B.Lipkowitz, D.B.boyd; 'Reviews in Computational Chemistry', Ch.9, (1992).
- [16] A.Klamt, G.Schuurmann; J.Chem.Soc.Perkin Trans., **2**, 799 (1993).
- [17] A.K.Ghose et al.; J.Comput.Chem., **9**, 80 (1988).